Original Article

Hypoxic mesenchymal stem cell secretome upregulates *IL-10* and *STAT3* gene expressions in mice model with polycystic ovary syndrome

Lusiana Lusiana[1], Dewi M. Darlan[2], Setyo Trisnadi[3], Agung Putra[3,4,5], Nur D. Amalina[5,6*] and Sofian A. Husain[5]

[1]Postgraduate Program, Faculty of Medicine, Universitas Islam Sultan Agung, Semarang, Indonesia; [2]Department of Parasitology, Faculty of Medicine, Universitas Sumatera Utara, Medan, Indonesia; [3]Department of Pathology, Faculty of Medicine, Universitas Islam Sultan Agung, Semarang, Indonesia; [4]Department of Postgraduate Biomedical Science, Faculty of Medicine, Universitas Islam Sultan Agung, Semarang, Indonesia; [5]Stem Cell and Cancer Research Indonesia, Semarang, Indonesia; [6]Department of Pharmacy, Faculty of Medicine, Universitas Negeri Semarang, Semarang, Indonesia

*Corresponding author: amalinadina2702@gmail.com

Abstract

Polycystic ovary syndrome (PCOS) is a condition characterized by chronic anovulation and hyperandrogenism, which often leads to infertility. It is closely associated with chronic inflammation triggered by glucose and saturated fat, contributing to hyperandrogenism and negatively impacting a patient's quality of life. Effective therapeutic approaches are essential to address these issues. The secretome of mesenchymal stem cells (MSCs) have demonstrated the ability to suppress pro-inflammatory cytokine secretion and regulate growth factors. The aim of this study was to investigate the effect of hypoxic mesenchymal stem cell secretome (MHSSCs) on the expression of *interleukin-10* (*IL-10*) and *signal transducer and activator of transcription 3* (*STAT3*) genes in a PCOS-induced mouse model. An in vivo experimental study was conducted using a post-test-only control group design. A total of 24 female C57BL/6 mice were divided into four groups: healthy control, negative control (PCOS mice injected with 0.9% NaCl), T1 (PCOS mice administered 200 µL of MHSSCs), and T2 (PCOS mice administered 400 µL of MHSSCs) for 33 days. Gene expression of *IL-10* and *STAT3* were quantified using quantitative reverse transcription polymerase chain reaction (qRT-PCR), normalized to the expression of the housekeeping β-actin gene. Statistical analysis using one-way ANOVA followed by the least significant difference (LSD) post-hoc test was then performed. The results showed a significant increase in *IL-10* expression in the T2 group compared to the negative control group ($p<0.001$). *STAT3* expression was also significantly higher in the T2 group compared to the negative control group ($p=0.035$). A dose-dependent effect was observed, with the T2 group demonstrating the highest upregulation of both *IL-10* and *STAT3* expression levels. The study highlights that the administration of MHSSCs effectively increased *IL-10* and *STAT3* gene expression, suggesting their potential as a therapeutic strategy to alleviate inflammation in PCOS.

Keywords: Polycystic ovary syndrome, mesenchymal stem cells, hypoxic secretome, IL-10, STAT3

Introduction

Polycystic ovary syndrome (PCOS) is a prevalent endocrine disorder affecting reproductive-aged women, characterized by hyperandrogenism, anovulation, and polycystic ovaries [1]. The

Received: November 23, 2024 - Accepted: December 28, 2024 - Published online: December 31, 2024

syndrome is associated with a range of metabolic and hormonal disturbances, including irregular menstrual cycles, hirsutism, insulin resistance, and an increased risk of metabolic comorbidities such as obesity and type 2 diabetes mellitus [2]. Recent advances in regenerative medicine have highlighted the potential of stem cell-based therapies in addressing the complex pathophysiology of PCOS. Among these, mesenchymal stem cells (MSCs) have gained attention for their self-renewal and differentiation capabilities, showing promise in restoring ovarian function and mitigating metabolic imbalances associated with PCOS [3].

Notably, hypoxic preconditioning of MSCs has emerged as a strategic approach to enhance their therapeutic potential [4]. Hypoxic conditions mimic the microenvironment of injured tissues, inducing the secretion of a bioactive secretome enriched with cytokines, growth factors, and anti-inflammatory molecules. This hypoxia-conditioned secretome exhibits superior regenerative and immunomodulatory properties compared to conventionally cultured MSCs [5]. The dynamic interplay between pro-inflammatory and anti-inflammatory factors plays a crucial role in PCOS pathogenesis. Interleukin (IL)-10 regulates immune responses by suppressing pro-inflammatory signaling pathways, such as nuclear factor kappa B (NF-κB) activation [6]. This suppression reduces the production of cytokines like IL-6 and tumor necrosis factor-α (TNF-α), which are elevated in PCOS and contribute to chronic inflammation and ovarian dysfunction [6]. Similarly, the signal transducer and activator of transcription 3 (STAT3) is a transcription factor that affects cellular processes, including inflammation, survival, and proliferation. In PCOS, *STAT3* gene is often dysregulated. STAT3 activation, typically induced by IL-10 through Janus kinase-signal transducer and activator of transcription (JAK-STAT) signaling, enhances the expression of genes like suppressor of cytokine signaling 3 (*SOCS3*), which further suppress inflammatory cascades and promote ovarian repair and function [7,8].

Despite these promising insights, the specific impact of mesenchymal hypoxia secretome stem cells (MHSSCs) on the expression of *IL-10* and *STAT3* gene in PCOS remains inadequately explored. MHSSCs represent an emerging therapeutic approach, characterized by a secretome enriched with bioactive factors under hypoxic conditions, which may provide enhanced regenerative and immunomodulatory properties compared to conventionally cultured MSCs [9,10]. The aim of this study was to investigate the effects of MHSSCs on the expression profiles of *IL-10* and *STAT3* genes in a PCOS animal model.

Methods

Study design

This study was designed as a true experimental post-test-only study, and was conducted in compliance with ethical standards. The experimental study design was developed to ensure a minimum error degree of freedom of 15. The sample size was calculated using the Federer formula to meet the statistical power requirements. Groups included healthy control, negative control (PCOS-induced), and PCOS mice treated with MHSSCs. No blinding was performed, and all experimental procedures were standardized to minimize variability. The animals were acclimatized for seven days before the study in a controlled environment, and interventions were conducted at the same time period each day to reduce diurnal variation.

Mesenchymal stem cells (MSCs) isolation and validation

Umbilical cord blood was collected and mononuclear cells were isolated by density gradient centrifugation using Ficoll-Paque Plus (GE Healthcare, USA). The isolated cells were cultured in T-75 flasks containing low-glucose Dulbecco's modified eagle medium (DMEM) (Gibco, USA) supplemented with 10% fetal bovine serum (FBS) (Gibco, USA) and 1% penicillin-streptomycin (Gibco, USA). Cultures were maintained at 37°C in a humidified atmosphere with 5% CO_2. Cells were passaged at 80–90% confluence using TrypLE Express (Gibco, USA).

At passage 3, MSCs were harvested, counted, and resuspended in phosphate-buffered saline (PBS) supplemented with 2% FBS. The cells were incubated with anti-human CD73, CD90, CD105, CD34, CD45, and HLA-DR antibodies (BD Biosciences, USA) for 30 minutes at 4°C. After washing, flow cytometry analysis was performed using a BD Accuri C6 Flow Cytometer (BD Biosciences, USA). Adipogenic differentiation was assessed by culturing passage 4 MSCs in

Adipogenic Induction Medium (Gibco, USA) for 21 days, followed by Oil Red O staining to visualize lipid droplets. Osteogenic differentiation was evaluated by culturing the cells in Osteogenic Induction Medium (Gibco, USA) for 21 days, followed by Alizarin Red staining to detect calcium deposits.

Induction of hypoxia in MSCs

Passage 5 MSCs were exposed to hypoxic conditions (5% oxygen) in a hypoxia chamber (Stemcell Technologies, Canada) for 24 hours, while control cells were maintained under normoxic conditions (21% oxygen). The hypoxia medium was collected after 24 hours, filtered, and stored at -80°C for subsequent analyses. The oxygen concentration in the hypoxia chamber was monitored continuously. The resultant hypoxic MSCs were labeled as MHSSCs. Additional details of the hypoxia induction protocols are provided elsewhere [11].

Animal model and PCOS induction

The PCOS model was established following previously published protocols [12]. Briefly, adult female C57BL/6 mice (n=24), confirmed to be in healthy condition, were used. Mice were housed in a temperature-controlled room (22–24°C) with a 12-hour light-dark cycle and had ad libitum access to standard rodent chow and water. PCOS was induced by daily subcutaneous injections of dehydroepiandrosterone (DHEA) (Sigma-Aldrich, USA) dissolved in sesame oil (6 mg/100 g body weight) for 30 days. Control animals received sesame oil alone without DHEA.

Testosterone quantification by ELISA

Serum testosterone levels were quantified using a Mouse Testosterone ELISA kit (Enzo Life Sciences, USA) according to the manufacturer's instructions. Standards, controls, and serum samples (50 µL each) were loaded in duplicate onto a microplate pre-coated with testosterone-specific antibody. Plates were incubated at 37°C for 60 minutes, followed by washing three times with the provided wash buffer to remove unbound components. A testosterone-horseradish peroxidase (HRP) conjugate was then added (50 µL per well) and incubated for 30 minutes at 37°C. Following another washing step, 100 µL of the substrate solution was added to each well and allowed to react for 20 minutes in the dark at room temperature. The reaction was terminated by adding 50 µL of stop solution, and absorbance was measured at 450 nm using a microplate reader (BioTek, USA). Testosterone concentrations were calculated by plotting absorbance values against a standard curve generated using known testosterone concentrations (0.1–25 ng/mL).

Validation of PCOS by estrus cycle analysis

Mice were euthanized on day 23 following the completion of experiments using a protocol compliant with ethical guidelines. Euthanasia was performed via intraperitoneal injection of sodium pentobarbital (50 mg/kg) to ensure humane treatment. Following euthanasia, ovaries were carefully excised, fixed in 10% formalin, and embedded in paraffin for histological analysis. Paraffin-embedded ovarian sections (5 µm thick) were deparaffinized, rehydrated, and stained with hematoxylin for 5 minutes. After rinsing, sections were counterstained with eosin for 1 minute, followed by dehydration and cover-slipping. Hematoxylin and eosin (HE)-stained sections were examined under a light microscope (Olympus BX53, Japan) by a blinded observer. Estrus cycle phases (proestrus, estrus, metestrus, and diestrus) were identified based on ovarian morphology, vaginal epithelial characteristics, and leukocyte infiltration.

Administration of MHSSCs in PCOS model

DHEA injections were continued subcutaneously until day 30 to prevent ovarian self-recovery. Simultaneously, MHSSCs were administered intraperitoneally from day 23 to day 30, with doses of 200 µL (called treatment 1 (T1) group) and 400 µL (called treatment 2 (T2) group) on days 23, 25, 28, and 30. The MHSSCs were suspended in PBS supplemented with 2% FBS before administration. The negative control group received intraperitoneal injections of PBS alone. Groups were clearly labeled to ensure accurate tracking and data attribution during the study. Estrus cycle phases were analyzed through cytological examination from day 27 to day 32. On day 33, testosterone levels were quantified, polymerase chain reaction (PCR) analyses were conducted, and ovarian samples from all groups were collected for histological observation.

Gene expression analysis by qRT-PCR

Ovarian tissues were harvested and homogenized, followed by total RNA extraction using TRIzol Reagent (Invitrogen, USA). cDNA was synthesized using SuperScript IV Reverse Transcriptase (Invitrogen, USA). Quantitative real-time PCR (qRT-PCR) was performed using PowerUp™ SYBR™ Green Master Mix (Applied Biosystems, USA) on a QuantStudio 3 Real-Time PCR System (Applied Biosystems, USA). Primer sequences for *IL-10* and *STAT3* were designed and validated (sequences available upon request). Relative expression levels were calculated using the ΔΔCt method, as previously recommended [13,14]. The target gene's Ct values were normalized to *β-actin* gene expression, followed by comparing these normalized values to a reference or control group.

Statistical analysis

Data normality was assessed using the Shapiro-Wilk test, and homogeneity of variances was verified using Levene's test. A p-value >0.05 indicated normal distribution and homogeneity of variances. Differences among treatment groups were analyzed using one-way ANOVA, with $p<0.05$ considered statistically significant, followed by least significant difference (LSD) post-hoc testing to identify pairwise group differences. Non-normally distributed data were analyzed using the Kruskal-Wallis and Mann-Whitney U tests as appropriate. Statistical analyses were performed using SPSS software (version 26, IBM, Armonk, New York, USA).

Results

MSCs isolation and its validation

Microscopic observation after passage 5 revealed adherent cells with a spindle-shaped morphology attached to the flask surface (**Figure 1**). Post-hypoxia, the MSCs exhibited denser growth compared to their appearance under normoxic conditions. The hypoxia-exposed MSCs expressed CD90 (97.60%) and CD29 (97.70%), while showing minimal expression of CD45 (1.50%) and CD31 (3.20%) (**Figure 1**). Differentiation assays demonstrated the potential of MHSSCs to mature into specific cell types (**Figure 1**). Under osteogenic conditions, the MHSSCs formed calcium deposits detectable by Alizarin Red staining, whereas adipogenic induction led to the formation of lipid droplets, visualized with Oil Red O staining (**Figure 2**).

Validation of PCOS animal model

Macroscopic observations revealed an increased number of palpable nodules in DHEA-induced mice compared to healthy mice, suspected to be follicular cysts, a characteristic sign of PCOS (**Figure 3**). Microscopic examination displayed the presence of cystic follicles, further confirming this characteristic. Administration of DHEA induction in mice resulted in elevated testosterone levels, confirming the development of PCOS (**Figure 3**).

MHSSCs induced IL-10 and STAT3 gene expression in PCOS animal model

Effects of MHSSCs on *IL-10* and *STAT3* gene expressions are presented in **Figure 4**. The T2 group exhibited a significant upregulation in *IL-10* gene expression compared to the control group ($p<0.001$). Similarly, the T2 group displayed a notable increase in *STAT3* gene expression compared to the control group ($p=0.035$). A dose-dependent relationship was observed, with the higher-dose group (T2 group) demonstrating a more pronounced upregulation of both *IL-10* and *STAT3* gene expression levels compared to the lower-dose group of MHSSCs (T1 group).

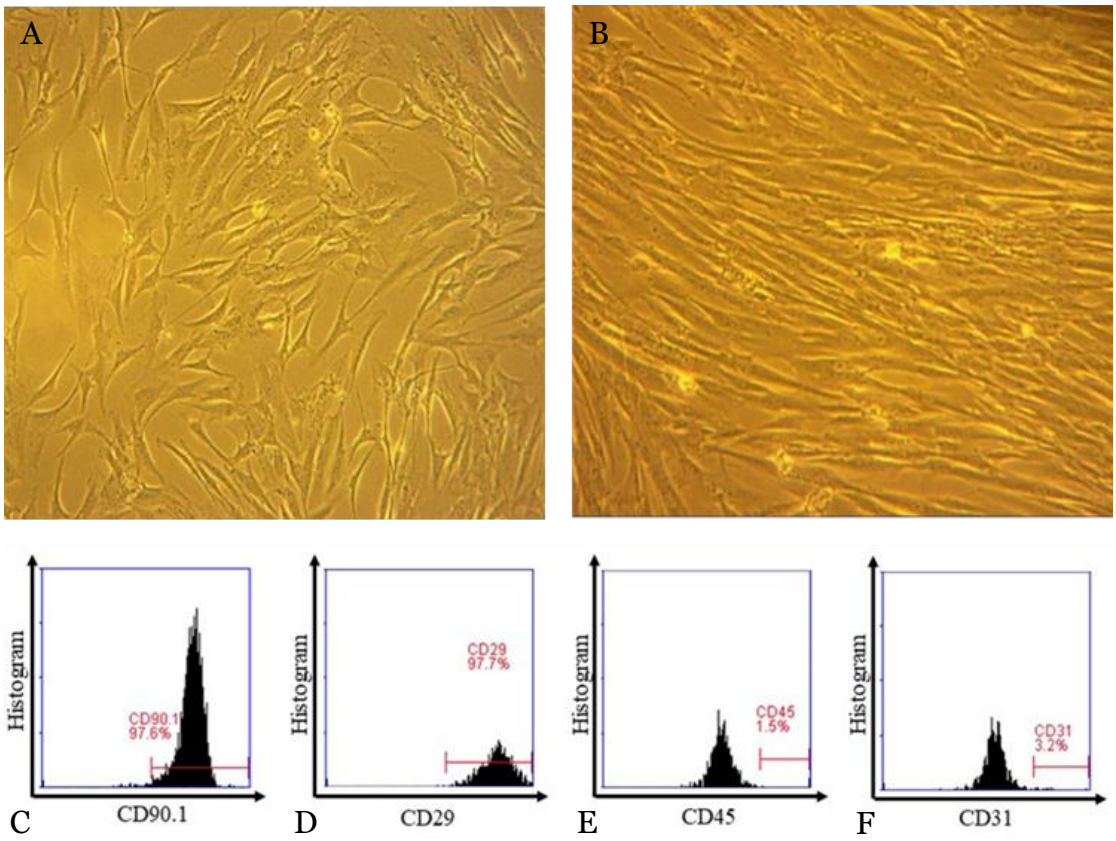

Figure 1. Microscopic photographs of isolated MSCs after passage 5 (A) and under hypoxic conditions (B). Flow cytometry histograms depicting the expression levels of surface markers CD90.1 (C), CD29 (D), CD45 (E), and CD31 (F). The percentage of positive cells is indicated for each marker.

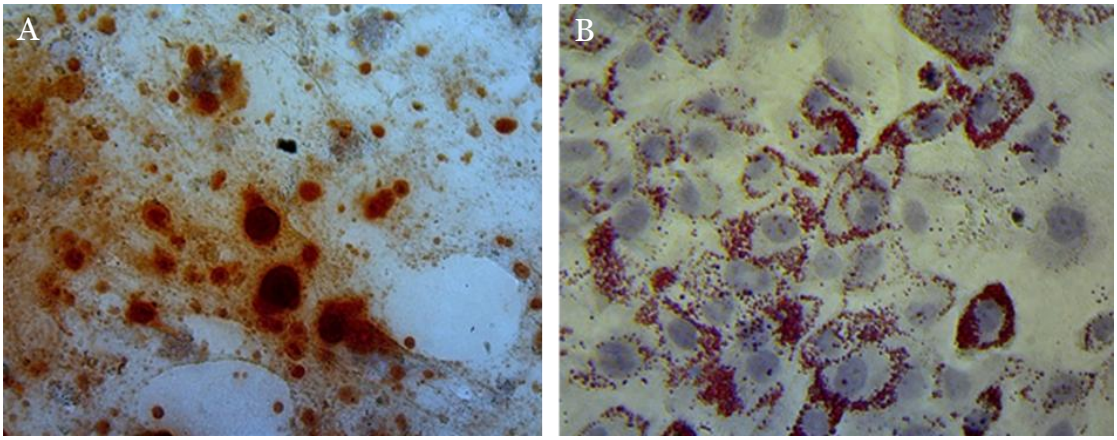

Figure 2. Osteogenic differentiation (A) and adipogenic differentiation (B) potential of MHSSCs as demonstrated by staining.

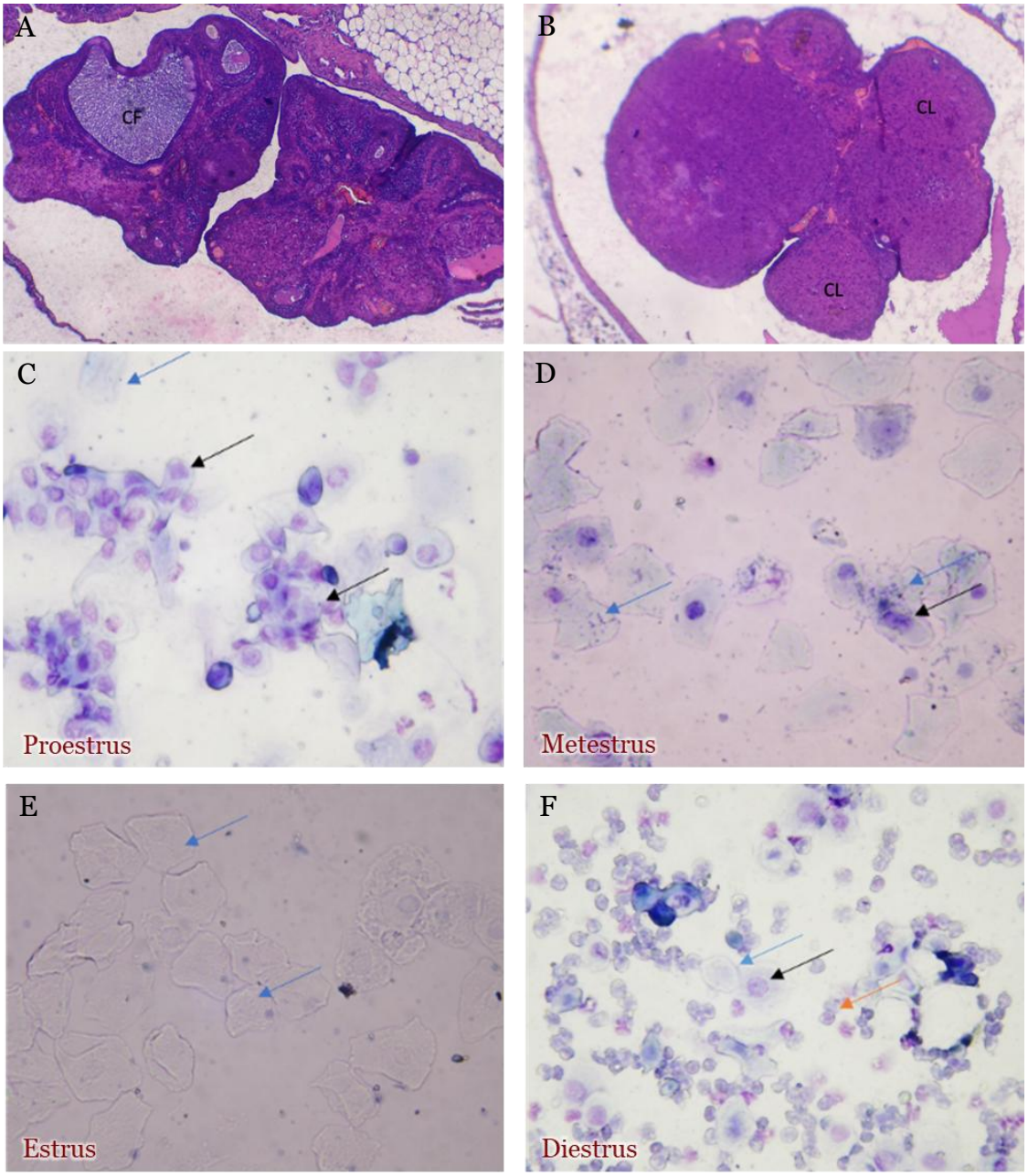

Figure 3. Microscopic images of palpable nodules in PCOS mice (A) and healthy mice (B), observed under HE staining at 100× magnification. Representative histological section of proestrus (C), metestrus (D), estrus (E), and diestrus (F) under HE staining. CL: corpus luteum; CF: cystic follicle.

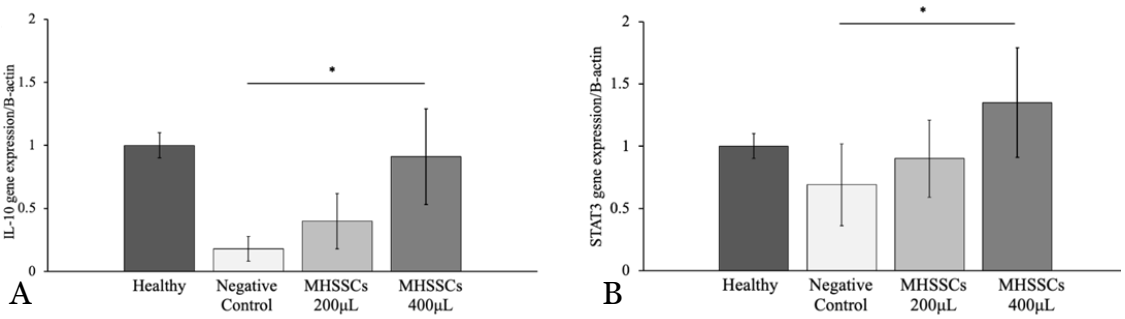

Figure 4. Gene expression ratio of (A) *IL-10* and (B) *STAT-3* after MHSSCs treatment on PCOS model under qRT-PCR analysis. The data represent the average and SD from three different independent experiments. The symbol * indicates significantly different at $p<0.05$.

Discussion

Findings from the present study revealed that the administration of MHSSCs significantly upregulated *IL-10* and *STAT3* gene expression in a dose-dependent manner, with the T2 group (400 µL dose of MHSSCs) showing higher levels compared to the T1 group (200 µL dose). This upregulation was associated with reduced inflammation in the PCOS model, likely mediated through macrophage polarization and inhibition of pro-inflammatory pathways. PCOS pathogenesis is closely linked to chronic ovarian inflammation, which disrupts follicular development and contributes to hyperandrogenism [15,16]. The elevated levels of IL-10 observed in this study are important for reducing inflammation in the ovarian microenvironment. IL-10 has been reported to block the activation of NF-κB [17], which is a major factor responsible for the production of pro-inflammatory cytokines like IL-6 and TNF-α.

Chronic inflammation occurs in the ovaries and surrounding tissues, marked by an abundance of type 1 macrophages (M1), which produce pro-inflammatory cytokines like IL-6, TNF-α, and IL-1β, thus perpetuating chronic inflammation [18,19]. A previous study showed that in some cases of PCOS, there is an imbalance between M1 activity and IL-10 levels [20]. Additionally, IL-10 can inhibit the Toll-like receptor signaling pathways pathway by suppressing phosphorylation of mitogen-activated protein kinase (MAPK) and TGF-beta-activated kinase 1 (TAK1), leading to reduced NF-KB activation induced by Toll-like receptor signaling. *IL-10* also inhibits the activity of tumor necrosis factor receptor-associated factor 6 (TRAF6), a critical mediator in NF-KB activation [21-23]. We stipulate that the MHSSCs could transform M1 into anti-inflammatory M2 macrophages. Differentiation of M1 into M2 balances the macrophage population within the ovaries, thereby halting the inflammatory process and reducing folliculogenesis [5].

The STAT3 pathway further complements this anti-inflammatory action of MHSSCs in the present study. The transcription factor STAT3 binds to the promoter region of genes regulating pro-inflammatory cytokine expression, inhibiting their transcription and thereby reducing pro-inflammatory cytokine production in chronic PCOS inflammation [24-26]. STAT3 plays a crucial role in regulating regulatory T cell (Treg) function, a key player in alleviating inflammation and maintaining immunological tolerance [15,27]. Activation of STAT3 in Treg enhances their ability to inhibit excessive immune responses and alleviate inflammation [28]. Moreover, STAT3 can direct macrophage differentiation towards the M2 phenotype, resulting in fewer pro-inflammatory cytokines and more anti-inflammatory cytokines, aiding in inflammation relief [15]. A study showed a decrease in inflammation through the activation of the IL-10-STAT3 pathways [15]. IL-10 binds to IL-10R, resulting in JAK 1 activation, inducing STAT3 phosphorylation [15]. The STAT3 protein translocate to the nucleus, activating mRNA SOSC3 sequences, which are then intracellularly expressed and can suppress pro-inflammatory signaling pathways, namely NF-κB [29,30]. Suppression of the NF-κB pathway leads to a decrease in pro-inflammatory cytokine secretion, including IL-6 [31]. Previous research utilizing fibrin-facilitated MSCs reported that MSCs regulate estradiol and progesterone, decrease gonadotropin, testosterone, and TGF-β1, maintain regular estrus cycles, increase granulosa cell counts, and decrease immature cystic follicles [32,33].

Overall, the findings provide compelling evidence for the anti-inflammatory and immunomodulatory potential of MHSSCs in PCOS management. However, this study has limitations that warrant consideration. The lack of analysis of pro-inflammatory cytokines, such as IL-6 and TNF-α, restricts a comprehensive understanding of the inflammatory pathways involved. Additionally, future studies should explore the long-term outcomes of MHSSC administration and its effects on hormonal regulation, follicular development, and ovarian morphology.

Conclusion

MHSSCs possess significant anti-inflammatory and immunomodulatory effects that are beneficial in PCOS management, as observed through the dose-dependent upregulation of *IL-10* and *STAT3* gene. Further research is required to explore the long-term efficacy, optimize dosing,

and assess the impact of MHSSCs on hormonal regulation and follicular development in the PCOS model.

Ethics approval

This study was approved by *Komisi Bioetik* Faculty of Medicine Universitas Islam Sultan Agung Semarang, Indonesia under No. 14/II/2024/Komisi Bioetik.

Acknowledgments

None.

Competing interests

All the authors declare that there are no conflicts of interest.

Funding

This study received no external funding.

Underlying data

Derived data supporting the findings of this study are available from the corresponding author on request.

Declaration of artificial intelligence use

We hereby confirm that no artificial intelligence (AI) tools or methodologies were utilized at any stage of this study, including during data collection, analysis, visualization, or manuscript preparation. All work presented in this study was conducted manually by the authors without the assistance of AI-based tools or systems.

How to cite

Lusiana L, Darlan DM, Trisnadi S, *et al*. Hypoxic mesenchymal stem cell secretome upregulates *IL-10* and *STAT3* gene expressions in mice model with polycystic ovary syndrome. Narra X 2024; 2 (3): e176 - https://doi.org/10.52225/narrax.v2i3.176.

References

1. Deswal R, Narwal V, Dang A, *et al.* The prevalence of polycystic ovary syndrome: A brief systematic review. J Hum Reprod Sci 2020;13(4):261-271.
2. Zuo T, Zhu M, Xu W. Roles of oxidative stress in polycystic ovary syndrome and cancers. Oxid Med Cell Longev 2016;2016.
3. Jee MK, Im YB, Choi JI, *et al.* Compensation of cATSCs-derived TGFβ1 and IL10 expressions was effectively modulated atopic dermatitis. Cell Death Dis 2013;4(2):1-13.
4. Putra A, Widyatmoko A, Ibrahim S, *et al.* Case series of the first three severe COVID-19 patients treated with the secretome of hypoxia-mesenchymal stem cells in Indonesia. F1000Res 2021;10:1-9.
5. Chugh RM, Park H soo, El Andaloussi A, *et al.* Mesenchymal stem cell therapy ameliorates metabolic dysfunction and restores fertility in a PCOS mouse model through interleukin-10. Stem Cell Res Ther 2021;12(1).
6. You M, Wang Z, Kim HJ, *et al.* Pear pomace alleviated atopic dermatitis in NC/Nga mice and inhibited LPS-induced inflammation in RAW 264.7 macrophages. Nutr Res Pract 2022;16(5):577-588.
7. Dace DS, Khan AA, Kelly J, *et al.* Interleukin-10 promotes pathological angiogenesis by regulating macrophage response to hypoxia during development. PLoS One 2008;3(10):e3381.
8. Tan W, Zou JL, Yoshida S, *et al.* Increased vitreal levels of interleukin-10 in diabetic retinopathy: A meta-analysis. Int J Ophthalmol 2020;13(9):1477-1483.
9. Silvana S, Japardi I, Rusda M, *et al.* Secretome from hypoxic mesenchymal stem cells as a potential therapy for ischemic stroke: Investigations on VEGF and GFAP expression. Narra J 2024;4(3):e1181.
10. Habibie YA, Emril DR, Azharuddin A, *et al.* Effect of umbilical cord mesenchymal stem cells on hypoxia-inducible factor-1 alpha (HIF-1α) production in arteriovenous fistula (AVF) animal model: A preliminary study. Narra J 2023;3(3):e225.

11. Sunarto H, Trisnadi S, Putra A, *et al.* The role of hypoxic mesenchymal stem cells conditioned medium in increasing vascular endothelial growth factors (VEGF) levels and collagen synthesis to accelerate wound healing. Indones J Cancer Chemoprevent 2020;11(3):134.
12. Xie Q, Xiong X, Xiao N, *et al.* Mesenchymal stem cells alleviate DHEA-induced polycystic ovary syndrome (PCOS) by inhibiting inflammation in mice. Stem Cells Int 2019;9782373
13. Putra A, Alif I, Nazar MA, *et al.* IL-6 and IL-8 Suppression by bacteria-adhered mesenchymal stem cells co-cultured with PBMCs under TNF-α exposure. Scitepress; 2021.
14. Restimulia L, Ilyas S, Munir D, *et al.* The CD4+CD25+FoxP3+ regulatory t cells regulated by MSCs suppress plasma cells in a mouse model of allergic rhinitis. Med Arch 2021;75(4):256-261.
15. Wang H, Feng X, Wang T, *et al.* Role and mechanism of the p-JAK2/p-STAT3 signaling pathway in follicular development in PCOS rats. Gen Comp Endocrinol 2023;330.
16. Guruvaiah P, Govatati S, Reddy TV, *et al.* The VEGF +405 G>C 5' untranslated region polymorphism and risk of PCOS: A study in the South Indian women. J Assist Reprod Genet 2014;31(10):1383-1389.
17. Baumann D, Drebant J, Hägele T, *et al.* P38 MAPK signaling in M1 macrophages results in selective elimination of M2 macrophages by MEK inhibition. J Immunother Cancer 2021;9(7).
18. Miki S, Suzuki JI, Takashima M, *et al.* S-1-Propenylcysteine promotes IL-10-induced M2c macrophage polarization through prolonged activation of IL-10R/STAT3 signaling. Sci Rep 2021;11(1).
19. Liu YC, Zou XB, Chai YF, *et al.* Macrophage polarization in inflammatory diseases. Int J Biol Sci 2014;10(5):520-529.
20. Chugh RM, Park HS, Esfandyari S, *et al.* Mesenchymal stem cell-conditioned media regulate steroidogenesis and inhibit androgen secretion in a PCOS cell model via BMP-2. Int J Mol Sci 2021;22(17).
21. Ridley AJ. Rho GTPases and actin dynamics in membrane protrusions and vesicle trafficking. Trends Cell Biol 2006;16(10):522-529.
22. Cho KA, Lee JK, Kim YH, *et al.* Mesenchymal stem cells ameliorate B-cell-mediated immune responses and increase IL-10-expressing regulatory B cells in an EBI3-dependent manner. Cell Mol Immunol 2017;14(11):895-908.
23. Saraiva M, O'Garra A. The regulation of IL-10 production by immune cells. Nat Rev Immunol 2010;10(3):170-181.
24. Ai XY, Qin Y, Liu HJ, *et al.* Apigenin inhibits colonic inflammation and tumorigenesis by suppressing STAT3-NF-κB signaling. Oncotarget 2017;8(59):100216-100226.
25. Lee H, Pal SK, Reckamp K, *et al.* STAT3: A target to enhance antitumor immune response. Curr Top Microbiol Immunol 2010;344:41-59.
26. Maliqueo M, Sundström PI, Vanky E, *et al.* Placental STAT3 signaling is activated in women with polycystic ovary syndrome. Hum Reprod 2015;30(3):692-700.
27. Maliqueo M, Sundström PI, Vanky E, *et al.* Placental STAT3 signaling is activated in women with polycystic ovary syndrome. Hum Reprod 2015;30(3):692-700.
28. Abdelhamed S, Ogura K, Yokoyama S, *et al.* AKT-STAT3 pathway as a downstream target of egfr signaling to regulate PD-l1 expression on NSCLC cells. J Cancer 2016;7(12):1579-1586.
29. Shi J, Li J, Guan H, *et al.* Anti-fibrotic actions of interleukin-10 against hypertrophic scarring by activation of PI3K/AKT and STAT3 signaling pathways in scar-forming fibroblasts. PLoS One 2014;9(5):e98228.
30. Xu Y, Tong Y, Ying J, *et al.* Chrysin induces cell growth arrest, apoptosis, and ER stress and inhibits the activation of STAT3 through the generation of ROS in bladder cancer cells. Oncol Lett 2018;15(6):9117-9125.
31. Lu YC, Wang P, Wang J, *et al.* PCNA and JNK1-Stat3 pathways respectively promotes and inhibits diabetes-associated centrosome amplification by targeting at the ROCK1/14-3-3σ complex in human colon cancer HCT116 cells. J Cell Physiol 2019;234(7):11511-11523.
32. Liu M, Yang SC, Sharma S, *et al.* EGFR signaling is required for TGF-β1-mediated COX-2 induction in human bronchial epithelial cells. Am J Respir Cell Mol Biol 2007;37(5):578-588.
33. Masyithah DD, Munir D, Karmila Jusuf N, *et al.* In vitro regulation of IL-6 and TGF-ß by mesenchymal stem cells in systemic lupus erythematosus patients. Med Glas 2020;17(2):408-413.